J. Mol. Model. **1997**, *3*, 117 – 123

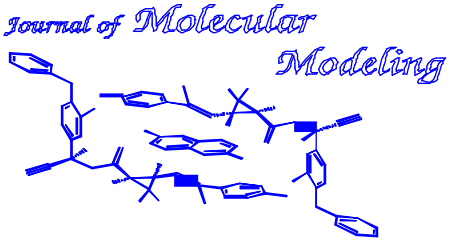

Molecular Modeling of Immunoglobulin Superfamily Proteins: Predicting the Three Dimensional Structure of the Extracellular Domain of CTLA-4 (CD152)

Jürgen Bajorath*[,1,2] and Peter S. Linsley[1]

[1]Bristol-Myers Squibb Pharmaceutical Research Institute, 3005 First Avenue, Seattle, WA 98121, USA;
Tel: (206) 727-3612; Fax: (206) 727-3602 (bajorath@protos.bms.com)

[2]Department of Biological Structure, University of Washington, Seattle, WA 98195.

Received: 5 December 1996 / Accepted: 3 February 1997 / Published: 21 February 1997

Abstract

The interactions between CD28/CTLA-4 (CD152) on T cells and their ligands CD80/CD86 on antigen presenting cells provide costimulatory signals critical for T cell activation. CD28/CTLA-4 and CD80/CD86 are members of the immunoglobulin superfamily (IgSF). CD28 and CTLA-4 both contain a single extracellular immunoglobulin (Ig) domain which binds CD80/CD86. Here we report modeling studies on the three-dimensional (3D) structure of the CTLA-4 binding domain. Since CTLA-4 displays only very weak sequence homology to proteins with known 3D structure, conventional modeling techniques were difficult to apply. Structure-oriented sequence comparison, consensus residue analysis, conformational searching, and inverse folding calculations were employed to aid in the generation of a comparative CTLA-4 model. Regions of high and low prediction confidence were identified, and the sequence-structure compatibility of the model was determined. Characteristics of the modeled structure, which resembles an Ig V domain, were analyzed, and the model was used to map N-linked glycosylation sites and residues critical for CTLA-4 function. The modeling approach described here can be applied to predict 3D structures of other IgSF proteins.

Key words: Immunoglobulin superfamily, protein structure prediction, sequence-structure analysis, comparative modeling, model assessment

Introduction

T cell activation is critically dependent on the presence of costimulatory signals which complement T cell receptor engagement by peptide-MHC complexes [1]. The interaction between CTLA-4 (CD152) and CD28 on T cells and CD80 and CD86 on antigen presenting cells is essential for effective costimulation [1]. CD28 and CTLA-4 are, like CD80 and CD86, members of the immunoglobulin superfamily (IgSF) and contain a single Ig-like extracellular domain. On the cell surface, both CTLA-4 and CD28 form homodimers via a disulfide link in the stalk region, and each monomer contains a binding site for CD80/CD86 [2]. In solution, these

* *To whom correspondence should be addressed*

domains are predominantly monomeric and bind CD80/CD86 with 1:1 stoichiometry [2].

The sequence of the extracellular domain of CTLA-4 shows IgSF characteristics [3], and we have previously generated a structural outline of this domain to aid in the rationalization and design of mutagenesis studies [4]. The major conclusions of this study were that the conserved M99-Y-P-P-P-Y104 motif in CTLA-4 and CD28, which is critical for function, maps to the loop connecting β-strands F and G (F-G loop) and that residues in the spatially adjacent B-C loop, which is not conserved, modulate binding avidity [4]. The F-G and B-C loops in CTLA-4 correspond to the antibody Complementarity Determining Region (CDR) loops 3 and 1, respectively [2]. In antibodies, CDR loops 1-3 of both variable heavy and light chains determine antigen specificity. While this study has been useful to explain and guide mutagenesis experiments, it has not allowed to analyze structural details of CTLA-4 beyond the level of an outline structure. More detailed structural predictions by comparative modeling were difficult, since CTLA-4 displays only very weak sequence identity with other (IgSF) proteins of known 3D structure, and were initially not attempted.

We have now, while the solution structure of monomeric extracellular domain of CTLA-4 is being determined (W. Metzler & L. Mueller, personal communication), attempted a more detailed prediction of the 3D structure of CTLA-4 to provide a complete molecular model. The study provides an example for modeling of IgSF proteins in the presence of low sequence similarity and the basis for a subsequent assessment of modeling accuracy. Details of the modeling approach are presented herein.

CTLA-4 sequences from different species were analyzed in light of IgSF consensus residue patterns and a topological alignment of representative structures. Sequence segments in CTLA-4 which could be assigned with confidence to Ig framework β-strands were identified, and alternative alignments were produced for lower confidence regions. A core region model was built using a V-domain template and complemented with loop conformations generated by conformational search or modeled based on backbone templates. Models based on alternative local sequence alignments were tested by inverse folding analysis. The refined model was used to predict structural characteristics of CTLA-4 beyond the backbone level and to map residues critical for CD80/CD86 binding.

Methods

Sequence searches in the Brookhaven Protein Data Bank were performed via the GeneQuest internet server. CTLA-4 sequences from different species were aligned using the Pileup routine of GCG (Genetics Computer Corp., Madison, WI). The alignment was combined with a topological sequence alignment including the structures of the antibody variable light (VL) chain of REI [5], the variable heavy chain of KOL [6], and the V-domain of CD8 [7]. This alignment was based on backbone superposition of framework β-strands in these structures. The alignments were combined by matching IgSF consensus residue positions [8, 9]. Core regions of the VL domain of REI were selected as template structure for modeling.

Computer graphics and model building were carried out using InsightII (MSI, San Diego, CA). Side chain replacements were modeled by low energy rotamer search [10]. The A'-B, D-E, and E-F loops were modeled based on the corresponding loop backbone conformations of REI, and the C'-D loop based on the corresponding loop conformation of CD8. Steric strain at loop splice points was relieved by energy minimization.

Other loop conformations were modeled by CONGEN conformational search [11]. These loops were modeled in the following order: F-G/CDR3-analogous loop (residues 98-105); C'-C"/CDR2-analogous loop (52-55); B-C/CDR1-analogous loop (partial search: 25-32, complete search: 25-30); C-C' loop (40-44). For each loop, conformations with negative potential energy were sampled and superposed. Similar conformations (maximum backbone rmsd ~1 Å) were identified and of these, the lowest energy conformation was selected. This selection protocol was applied to screen loop conformations not only based on force field energy but also on probability. In the final model, side chain conformations of residues in CONGEN-modeled loops were adjusted to similar rotamer conformations using InsightII.

The initially assembled model was refined by conjugate gradients energy minimization with Discover (MSI, San Diego, CA). In these calculations, AMBER [12] force field parameters were used, and a distance-dependent dielectric constant (1r) and a 10 Å cutoff distance for non-bonded interactions were applied. During minimization, backbone constraints of initially 100 kcal/Å^2 (1 kcal = 4.18 kJ) were gradually released, and unconstrained minimization was continued until the rmsd of the energy function was ~1 kcal/Å. At this stage, the backbone rmsd between the initial and the refined model was less than 1 Å. The stereochemistry of the model was examined using Procheck [13].

The sequence-structure compatibility of the model was analyzed using the ProsaII 3.0 energy profile method [14]. For graphical representation of the energy profiles, a 50 residue window was used for energy averaging at each residue position [14]. Energy profiles were plotted using ProsaII. Color figures were produced using InsightII and processed as RGB images.

Results and Discussion

CTLA-4 displays less than 20% sequence identity to proteins with available 3D structure. At this low level, evolutionary relationships, which establish structural similarity, are unclear [9, 15]. The suggestion that CTLA-4 belongs to the IgSF came from the presence of two cysteine residues

```
           1 # #   #    *    15
huCTLA-4: -MHVAQ-  PAVVLAS SRG
rbCTLA-4: -LHVSQ-  PAVVLAS SRG
raCTLA-4: -IQVTQ-  PAVVLAS SHG
muCTLA-4: -IQVTQ-  PAVVLAS SHG
REI VL  : DIQMTQS  PSSLSAS VGD
KOL VH  : EVQLVQS  GG-GVVQ PGR
CD8     : -SQFRVS  PLDRTWN LGE
            (A)      (A')
           -------    -----


              # # 5 #    *     15 # * *    25        # *  *40
huCTLA-4: ---MHVAQ PA-VVLA SSRG IASFVCEYA SPGKATEV RVTVLRQA DSQ---
rbCTLA-4: ---LHVSQ PA-VVLA SSRG VASFVCEYA SSHKATEV RVTVLRQA NSQ---
raCTLA-4: ---IQVTQ PA-VVLA SSHG VASFPCEYA SSHNTDEV RVTVLRQT NDQ---
muCTLA-4: ---IQVTQ PA-VVLA SSHG VASFPCEYS PSHNTDEV RVTVLRQT NDQ---
REI VL  : DIQMTQS- PSSLSAS VGD- RVTITCQAS QDIIK--- YLNWYQQT PGKA--
KOL VH  : EVQLVQS- GG-GVVQ PGR- SLRLSCSSS GFIFSSY- AMYWVRQA PGKG--
CD8     : -SQFRVS- PLDRTWN LGE- TVELKCQVL LSNPTS-- GCSWLFQP RGAAAS
            (A)      (A')          (B)              (C)
           --------   -----      ---------          --------


              ##       55        #  64** # 72       # * *   #  87
huCTLA-4: VTEVCAAT YMMG- NELT -FLDDS ICTGTS SG-- NQVNLTIQ GLRAMDT
rbCTLA-4: MTEVCAMT YTVE- NELT -FIDDS TCTGIS HG-- NKVNLTIQ GLSAMDT
raCTLA-4: VTEVCATT FTVK- NTLG -FLDDP FCSGTF NE-- SRVNLTIQ GLRAADT
muCTLA-4: MTEVCATT FTEK- NTVG -FLDYP FCSGTF NE-- SRVNLTIQ GLRAVDT
REI VL  : PKLLIYE- AS--- NLQA -GVPS- RFSGSG SG-- TDYTFTIS SLQPEDI
KOL VH  : PEWVAIIW DDGSD QHYA DSVKG- RFTISR NDSK NTLFLQMD SLRPEDT
CD8     : PTFLLYLS QNKP- KAAE -GLDTQ RFSGKR LG-- DTFVLTLS DFRRENE
            (C')         (C")          (D)         (E)
           --------       ----        -------     --------


           # * * #     101         106     * *118
huCTLA-4: GLYICKVE LMYPPPYY------ LGIGNGTQIYVI
rbCTLA-4: GLYICKVE LMYPPPYY------ VGMGNGTQIYVI
raCTLA-4: GLYFCKVE LMYPPPYF------ VGMGNGTQIYVI
muCTLA-4: GLYLCKVE LMYPPPYF------ VGMGNGTQIYVI
REI VL  : ATYYCQQY QSLP---------- YTFGQGTKLQIT
KOL VH  : GVYFCARD GGHGFCSSASCFGP DYWGQGTPVTVS
CD8     : GYYFCSAL SNSI---------- MYFSHFVPVFLP
            (F)                     (G)
           --------               ------------
```

Figure 1. *Structure-oriented alignment of CTLA-4 with representative IgSF V-domain structures. A topological alignment of the REI, KOL, and CD8 structures is shown. CTLA-4 sequences from different species (hu, human; rb, rabbit; ra, rat; mu, mouse) were included in the alignment by matching buried IgSF V-set consensus residues (*), additional core residues, and structurally constrained positions (#). Alternative alignments are shown for the A/A' strand in CTLA-4. Residue numbers are given for CTLA-4 according to reference 4 (i.e., S64 is followed by I67 and L106 by G108).*

(C21, C94) which are ~70 residues apart and surrounded by characteristic sequence patterns [3, 8]. **Figure 1** summarizes the structure-oriented sequence comparison on which modeling of CTLA-4 was based. An alignment of CTLA-4 sequences from different species was combined with a topological alignment of (related) IgSF structures. Details of these alignments are discussed below.

Sequence comparisons were based on IgSF consensus residues [8] and selected Ig structures. The prototypic Ig fold consists of two tightly packed β-sheets with 4 (ADEB) and 3 (GFC) or 5 (GFCC'C") strands, which are connected by loops

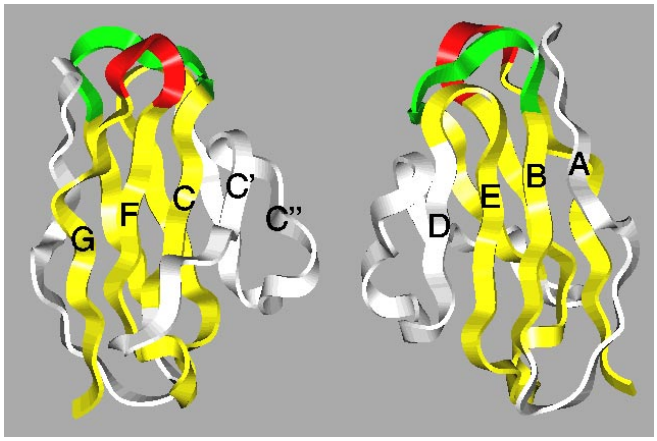

Figure 2. *Schematic representation of a representative Ig V-fold. β-strands are labeled. The left image focuses on the GFCC'C" β-sheet surface and the right image on the opposite ABED face. The B-C/CDR1-analogous loop and the F-G/CDR3-analogous loop are colored green and red, respectively. Core regions in CTLA-4 which could be predicted with high confidence (see text) are shown in yellow and lower confidence regions in white.*

following conserved topology [16]. However, IgSF molecules display significant variations in the number and spatial arrangement of β-strands and the length and conformations of loops [9, 17]. In many cases, structural variants can be classified as distinct IgSF structure types. These include, for example, V(ariable) and C(onstant) domains [8], S(witch)-type [9], or I(ntermediate)-set structures [17]. **Figure 2** shows a schematic representation of an Ig fold. Different Ig structure types are distinguished in part by the number of β-strands forming each sheet [16, 17]. For example, a C-domain lacks the C'- and C"-strands and an I-domain the C"-strand, both of which are found in V-type structures.

The conserved Ig cysteines, which are present in CTLA-4, are part of β-strands B and F. These two β-strands together with strands C and E form the core of the Ig fold, which is structurally conserved in IgSF molecules irrespective of their structure type [9]. The sequences corresponding to the B, C, E, F strands display highly conserved patterns of consensus residues which stabilize the core structure.

In accord with the above considerations, we first attempted to align CTLA-4 sequence segments to the conserved Ig core β-strands by matching IgSF signature residues (**Figure 1**). Only those consensus residues were considered which determine/stabilize the structures of single Ig domains and not domain dimerization [8]. The latter IgSF consensus residues map to exposed positions in monomeric Ig domains, do not stabilize the Ig fold, and are only relevant for the prediction of structures which show antibody-like dimerization such as, for example, CD8 [7].

In CTLA-4, the characteristic sequence patterns surrounding the Ig cysteines made the assignment of strands B and F unambiguous. The E-F loop is one of the most conserved loop regions in Ig domains. It is determined by a large hydrophobic packing residue at the second position in the loop and often a negatively charged residue at the sixth position, which is involved in an ionic interaction. This region preceding the F strand could also be assigned in CTLA-4 with confidence and, as a consequence, the alignment of the E strand was possible (**Figure 1**).

Many Ig domains include a highly conserved tryptophane core residue and a glutamine in the C strand. A glutamine but not the tryptophane residue was identified in CTLA-4. However, matching the glutamine position ensured that hydrophobic residues occupied the C-strand core residue positions (**Figure 1**). The alignment of the B and C strands also determined the size of B-C/CDR1-analogous loop (residues 25-32). Taken together, these findings suggested that sequence segments in CTLA-4 corresponding to the core regions of the Ig fold could be assigned with confidence.

The next question was whether CTLA-4 belongs to a known IgSF structure type, a prerequisite for comparative modeling [18]. Based on the core region alignment, 32 residues separate the C and E strands in CTLA-4, which clearly indicates the presence of a V-type fold [9] . This conclusion was further supported by the presence of one of two characteristic β-bulge sequence motifs, the (large hydrophobic)-G-X-G motif in the G-strand, which supports dimerization of a number of V-domains [7, 19]. In addition to these β-bulges, V-domain dimerization is supported by an array of hydrophobic/aromatic consensus residues on the A'GFCC'C" face (see above), which are not conserved in CTLA-4. The β-sheets of a prototypic V-fold consist of strands (ABED) and (GFCC'C") (**Figure 2)**. Based on the conclusion that CTLA-4 adopts a V-like fold, the alignment of CTLA-4 sequences was complemented by a topological alignment of representative V-type structures to support the structure-based analysis of sequence motifs.

Sequence segments in CTLA-4 remained to be assigned to putative β-strands A, D, C', C", and G. A confident alignment based on IgSF V-set consensus residues [8] was only possible for the G-strand. The G-strand in CTLA-4 contains a sequence segment (L-G-I-G-N-G) with two potential bulge region motifs (L-G-I-G and/or I-G-N-G). However, the requirement of two hydrophobic core residues at the C-terminal end of the strand was only consistent with a bulge formed by one of these motifs (I-G-N-G). The assignment of the F and G strands unambiguously mapped the M99-Y-P-P-P-Y104 motif in CTLA-4 to the CDR3- analogous loop.

Assignment of the remaining strands and loop regions was difficult since either sequence ambiguities existed (A, D) or IgSF consensus residues were absent (C', C"). To compensate for these difficulties, we have constructed intermediate models to inspect alternative alignments in three dimensions. In addition, alternative models were analyzed by energy profile analysis (see below). Since no template structure with clear sequence homology to CTLA-4 was available, the VL domain of REI [5], a representative V-fold, was selected as the starting point for modeling. First, the B, C, E,

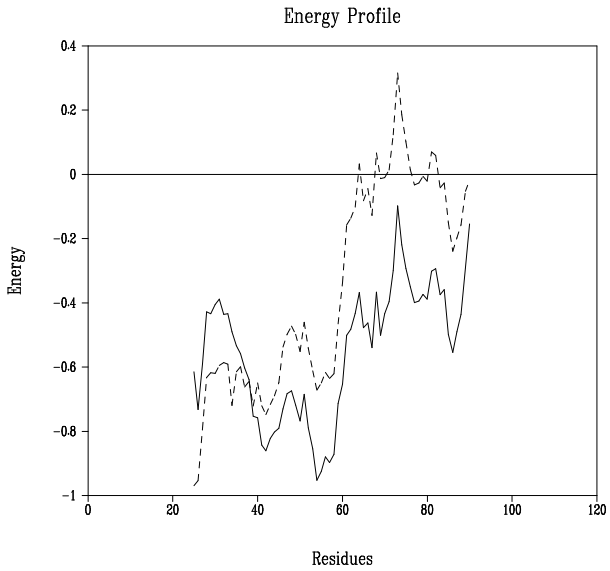

Figure 3. *Energy profile of alternative CTLA-4 models. The energy profiles were calculated with ProsaII using a 50 residue window for energy averaging at each position. Pairwise residue interaction energy is given in E/kT (E, interaction energy in kcal/mol (1 kcal = 4.18 kJ); k, Boltzmann constant; T absolute temperature in K). Energy profiles are compared for models with alternative A/A'-strand alignments (——, VL-like; ----, VH-like).*

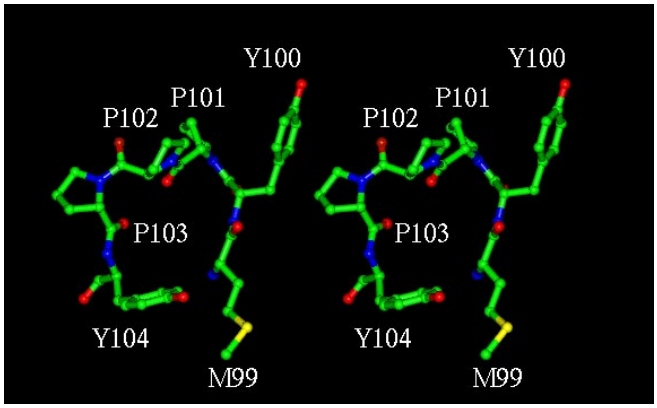

Figure 4. *Stereo view of the CDR3-analogous loop in CTLA-4. The M-Y-P-P-P-Y motif is critical for CTLA-4 function. Standard atom coloring is used (carbon, green; nitrogen, blue; oxygen, red; sulfur, yellow).*

F, G strands, which could be assigned with confidence, and intervening loops were modeled as described in the methods section. This core model was complemented by alternatively modeled regions, which could not be assigned with confidence based on sequence comparison alone.

In many V-type structures, the A strand is split (A+A') between the two β-sheets, which then consist of 4 (ABED) and 6 (A'GFCC'C") strands, respectively. The A-A' strand switch is usually marked by the presence of prolines or glycines. A proline is present at position 6 in CTLA- 4 and a strand switch was thus predicted. However, the three hydrophobic core residues in the A-A' region could be matched in alternative ways, which effectively changed the local alignment and the position of the strand switch. **Figure 1** includes 2 alternative alignments, both of which were plausible at the sequence level. One alternative is more consistent with the structure of VL, the other more consistent with VH domains. In the VL-like alignment, the residues V3, Q5, and A11 would be core residues. Alternatively, M1, V3, and L10 would occupy core positions.

To evaluate these possibilities, alternative models were built and analyzed by energy profile analysis [14]. This method belongs to the inverse folding approach [20] and is used to assess the sequence-structure compatibility of structural models, however obtained, based on statistically derived pairwise residue interaction energies [21]. Energy profile analysis has been shown to identify both global and local errors in protein structures [14]. **Figure 3** shows a comparison of the profiles of the two models with alternative A-A' alignments and structures. The lower average residue interaction energies indicate better sequence-structure compatibility for the model with VL-like alignment and A-A' transition, which was thus preferred.

Assignment of the D strand in CTLA-4 was difficult since the usually seen positively charged IgSF V-set consensus residue at the beginning of the strand is absent. This residue interacts with the E-F loop and is followed by a hydrophobic core residue, typically phenylalanine. The decision about this local alignment was supported by the finding that CTLA-4 contains an additional (non-Ig) intradomain disulfide bond (C48-C68) [22]. Therefore, C68, which maps to the D strand, must occupy a buried/core position. The most plausible alignment of the D-strand in human CTLA-4 placed I67 and C68 at the two IgSF consensus positions (**Figure 1**). Other alignments would have placed C68 at an exposed position or, alternatively, would be less compatible with the hydrophobic core of the domain. This alignment also matched a structurally constrained position (G70).

The V-domain C" strand at the edge of the β-sheet lacks structural stabilization by core residues and is often flexible. Similarly, the adjacent C'-strand has only two not rigorously conserved core positions. Due to this variability, it was difficult to produce a meaningful alignment for the C'-C" region in CTLA-4, which includes the CDR2-analogous loop. Energy profile analysis of models with alternative alignments in this region was inconclusive. Cysteine 48 of the non-Ig disulfide bond maps to the C'-C" region, and this finding aided in the alignment of the C' strand (**Figure 1**). This alignment was supported by computer graphical analysis of an intermediate model. At the selected position in the C' strand, the alpha carbon of C48 was within ~7 Å distance of the alpha carbon of C68 in the D strand (see above), compatible

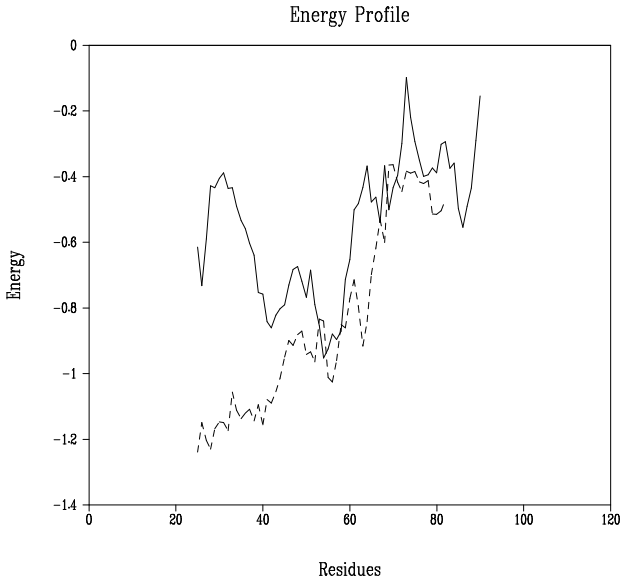

Figure 5. *Energy profile of the refined CTLA-4 model. The profile was generated as described in the legend of Figure 3. The energy profile of the model (——) is compared to the profile of the REI X-ray structure (----).*

with the formation of a disulfide bond. In addition, a hydrophobic residue was found in CTLA-4 at the preceding position. However, no preferred alignment could be found for the C" strand, as discussed above. As a consequence, the definition of the CDR2-analogous loop and the C"-D loop remained ambiguous. Therefore, a four residue C" strand and a five residue C"-D loop were modeled, as often seen in V-type domains, including REI.

Following the assignment of all β-strands and loops, the CTLA-4 core region model was completed. Considering loop size and sequence patterns, the conformations of four loops (A'-B, C'-D, D-E, E-F) were modeled based on loop conformations in other V-domains (see Methods). The model was then complemented by CONGEN-modeled loop conformations. The F-G/CDR3-analogous loop (L98-M-Y-P-P-P-Y104) loop is particularly important, since residues 99-104 are critical for CTLA-4 (and CD28) function, as assessed by alanine scanning mutagenesis [4]. **Figure 4** shows the modeled conformation of this loop, which is rigid due to the presence of three prolines. In the CONGEN-calculated CDR 3-analogous loop conformation, these proline residues (P101-P102-P103) were modeled in cis-trans-cis conformation.

The initially assembled model was refined by energy minimization, and the stereochemical quality of the improved model was confirmed. In **Figure 5**, a comparison of energy profiles of the CTLA-4 model and the REI VL domain, its structural template, is shown. The overall negative average residues interaction energies in the CTLA-4 model and the similarity of parts of the profiles indicate that the CTLA-4 model is sound and that significant errors in core regions of

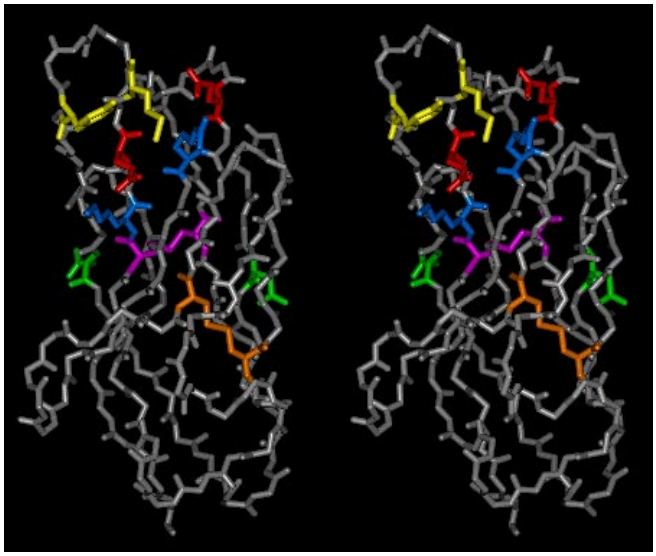

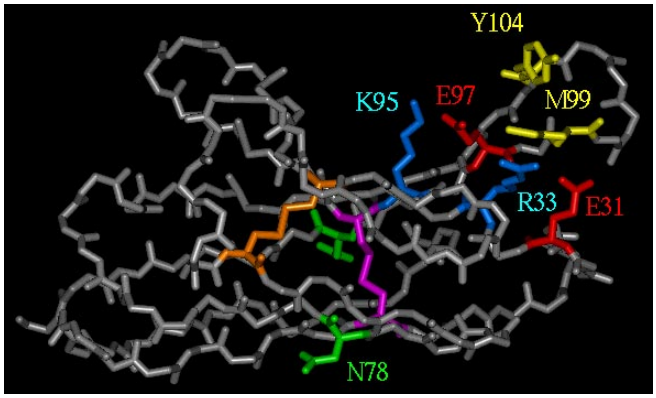

Figure 6. *The CTLA-4 model. The protein backbone of the model is shown in silver. Residues discussed in the text are mapped on the model and color-coded (hydrophobic, yellow; positively charged, blue; negatively charged, red; N-linked glycosylation sites, green; cysteines, gold/magenta). In* ***(a)****, a stereo view of the model is shown looking at the A'GFCC'C" face of the domain. In this orientation, the CDR-analogous loops are at the top. In* ***(b)****, a side view is shown. In this orientation, the CDR-analogous loops are on the right. The canonical Ig disulfide bond is shown in gold and the additional disulfide bond in magenta.*

the model are probably absent [14]. Thus, energy profile analysis suggested that the accuracy of the CTLA-4 model was sufficient to predict some structural details.

In **Figures 6a** and **6b**, the refined CTLA-4 model is shown in two different orientations to highlight some of its features. CTLA-4 includes two N-linked glycosylation sites, N78 in the E strand and N111 in the G strand. In the model, both sites are fully exposed. N111 is part of the conserved G strand β-bulge, and N78 maps to the center of the ABED β-sheet surface. The opposite A'GFCC'C" face displays several

charged residues on its surface (e.g., R33, E46, K95, E97). In contrast to antibody V-domains and CD8, these residues render the A'GFCC'C" face in CTLA-4 hydrophilic, which provides an explanation for the finding that CTLA-4 is stable as a monomer in solution. The modeled CDR3 analogous loop extends the accessible A'GFCC'C" surface. In addition to CDR3 residues, mutation of E31, R33 and K95, E97 in CTLA-4 has been shown to significantly reduce or abolish CD80/CD86 binding [23]. In the model, these four residues are exposed, map closely to CDR3 residues M99 and Y104, and form a coherent surface (**Figure 6**). In light of these findings, the F-G loop and residues on the A'GFCC'C" face are likely to form the ligand binding site in CTLA-4, similar to what has been observed for other IgSF members irrespective of the molecular nature of their ligands [24]. The mapping of N-linked glycosylation sites and residues critical for function to surface positions and the predicted spatial arrangement of these residues provides further support for the validity of the CTLA-4 model.

Conclusions

In this study, we have focused on the generation of a detailed CTLA-4 molecular model. CTLA-4 is representative for many IgSF proteins and members of other protein superfamilies as it shows only very limited sequence similarity to related molecules with known 3D structure. Thus, although the global fold may be predicted in these cases, the construction of a detailed and reliable model is difficult and requires the combination of different techniques. We have predicted that CTLA-4 adopts a V-like Ig fold and have shown how sequence segments were assigned to β-strands and loop regions. The importance of consensus residue analysis and structure-oriented sequence comparisons was emphasized and their limitations were illustrated. To generate a reasonable CTLA-4 model, core regions of high prediction confidence were built first and lower confidence regions were modeled subsequently. The model was assessed by energy profile analysis and in light of experimental findings. Taken together, these studies suggest that the quality of the model is sound. The CTLA-4 model is expected to include errors, for example, in loop and/or side chain conformations, but should be sufficiently accurate to predict core and surface residues and their spatial arrangement. This level of accuracy is required for meaningful applications of the model in protein engineering or other studies.

References

1. For review: Linsley, P. S.; Ledbetter, J. A. *Ann. Rev. Immunol.* **1993**, *11*, 191.
2. For review: Linsley, P. S.; Ledbetter, J.; Peach, R.; Bajorath, *J. Res. Immunol.* **1995**, *146*, 130.
3. Brunet, J. F.; Denizot, F.; Luciani, M. F.; Roux-Dosseto, M.; Suzan, M., Mattei, M. G.; Goldstein, P. *Nature* **1987**, *328*, 267.
4. Peach, R. J.; Bajorath, J.; Brady, W.; Leytze, G.; Greene, J.; Naemura, J.; Linsley, P. S. *J. Exp. Med.* **1994**, *180*, 2049.
5. Epp, O.; Lattman, E. E.; Schiffer, M.; Huber, R.; Palm, W. *Biochemistry* **1975**, *14*, 4943.
6. Marquardt, M.; Deisenhofer, J.; Huber, R.; Palm, W. *J. Mol. Biol.* **1980**, *141*, 369.
7. Leahy. D. J.; Axel, R.; Hendrickson, W. A. *Cell* **1992**, *68*, 1145.
8. For review: Williams, A. F.; Barclay, A. N. *Ann. Rev. Immunol.* **1988**, *6*, 381.
9. For review: Bork, P.; Holm, L.; Sander, C. *J. Mol. Biol.* **1994**, *242*, 309.
10. Bajorath, J.; Fine, R. M. *Immunomethods* **1992**, *1*, 137.
11. Bruccoleri, R. E.; Novotny, J. *Immunomethods* **1992**, *1*, 96.
12. Seibel, G.; Singh, U. C.; Weiner, P. K.; Caldwell, J.; Kollman, P. AMBER 3.0 revision A. San Francisco. University of California at San Francisco, **1990**.
13. Laskowski, R. A.; MacArthur, M. W.; Moss, D. S.; Thornton, J. M. *J. Appl. Cryst.* **1993**, *26*, 283.
14. Sippl, M. J. *Proteins: Structure, Function, and Genetics* **1993**, *17*, 355.
15. For review: Doolittle, R. F.; Bork, P. *Scientific American* **1993**, *269*, 50.
16. For review: Novotny, J.; Bajorath, J. *Adv. Prot. Chem.* **1996**, *49*, 149.
17. Harpaz, Y.; Chothia, C. *J. Mol. Biol.* **1994**, *238*, 528.
18. For review: Bajorath, J.; Stenkamp, R.; Aruffo, A. *Protein Science* **1993**, *2*, 1798.
19. Chothia, C.; Novotny, J.; Bruccoleri, R. A.; Karplus, M. *J. Mol. Biol.* **1985**, *186*, 651.
20. For review: Wodak, S. J.; Rooman, M. J. *Curr. Opin. Struct. Biol.* **199**3, *3*, 247.
21. For review: Sippl, M. J. *J. Comp.-Aided. Mol. Design* **1993**, *7*, 473.
22. Linsley, P. S.; Nadler, S. G.; Bajorath, J.; Peach, R. J.; Leung, H.; Rogers, J.; Bradshaw, J.; Stebbins, M.; Leytze, G.; Brady, W.; Malacko, A. R.; Marquardt, H.; Shaw, S.-Y. *J. Biol. Chem.* **1995**, *270*, 15417.
23. Morton, P. A.; Fu, X.-T.; Stewart, J. A;, Giacoletto, K. S.; White, S. L.; Leysath, C. E.; Evans, R. J.; Shieh, J.-J.; Karr, R. W. *J. Immunol.* **1996**, *156*, 1047.
24. For review: Skonier, J. E.; Bowen, M. A.; Emswiler, J.; Aruffo, A.; Bajorath, J. *Biochemistry* **1996**, *35*, 12287.